RESEARCH ARTICLE

$J2$-Aware Joint Optimization of Fuel Station Placement and Satellite Assignment for SSO Satellite Clusters

Tianle Yin[1,*], **Jiajing Zhu**[2], **Zheng Qiao**[3], **Shijie Xu**[3] **and Lei Zhao**[4]

[1] School of Aeronautics and Astronautics, Sun Yat-sen University, Shenzhen 518107, China
[2] Beijing Institute of Aerospace Control Devices, Beijing 100854, China
[3] School of Automation and Intelligent Science, Jiangnan University, Wuxi 214122, China
[4] National University of Defense Technology, Changsha 410073, China

Abstract

On-orbit refueling of sun-synchronous-orbit (SSO) satellite clusters requires effective deployment of fuel stations (FSs). To this end, this paper investigates the deployment optimization problem of fuel stations for SSO clusters by considering orbital geometry, satellite-to-station assignment, and refueling mission feasibility. A J_2-aware optimization framework is proposed, in which a particle swarm optimizer searches for optimal fuel-station orbital parameters and satellite assignments. For each candidate deployment, a deterministic mission evaluator is employed to estimate natural alignment opportunities, transfer requirements, and fuel consumption. The proposed approach considers the variation of the relative right ascension of the ascending node (RAAN) between the station and each target during the service interval, and evaluates transfer costs using both departure and terminal orbital geometries. A multi-objective optimization model is formulated to trade off propellant consumption, cluster balance, servicing-spacecraft requirements, and constraint violation penalty. Simulation results for a 20-target SSO cluster show that the optimized three-FS deployment serves all targets with a total refueling-related propellant consumption of 3405.8 kg and a total servicing-spacecraft requirement of four.

Keywords: on-orbit refueling, SSO, fuel-station placement, J_2 perturbation.

1 Introduction

1.1 Background and Motivation

Satellite clusters have become an important mission architecture for long-duration Earth-observation missions due to their advantages in coverage, redundancy, and mission flexibility [1, 2]; sustaining such clusters over extended horizons, however, requires addressing the orbital maintenance challenges introduced by J_2-induced perturbations [3]. Among these architectures, sun-synchronous-orbit (SSO) satellite clusters are widely adopted for Earth observation because of their stable lighting conditions and repeatable observation geometry [4, 5]; the distinctive orbital characteristics of SSO have also been exploited for multi-target

Submitted: 16 July 2026
Revised: 16 September 2026
Accepted: 21 September 2026
Published: 24 September 2026

Vol. 1, **No.** 3, 2026.
10.62762/AEC.2026.761344

***Corresponding author:**
✉ Tianle Yin
1895616670@163.com

Citation
Yin, T., Zhu, J., Qiao, Z., Xu, S., & Zhao, L. (2026). $J2$-Aware Joint Optimization of Fuel Station Placement and Satellite Assignment for SSO Satellite Clusters. *Aerospace Engineering Communications*, 1(3), 119–127.

mission planning within SSO [6]. On-orbit refueling provides a promising approach to extending mission lifetime without replacing the spacecraft [7, 8]; however, its effectiveness strongly depends on the deployment of fuel stations and the accessibility between servicing vehicles and target satellites [9–11].

The fuel-station (FS) placement problem for an SSO cluster couples orbital geometry, nodal precession, target fuel status, and service timing. The Earth's oblateness induces a secular drift of the right ascension of the ascending node (RAAN) [12], a phenomenon that has been exploited for constellation maintenance [13] and orbital facility placement [14]. The differential drift between a station and a target creates low-cost rendezvous opportunities, because a station can wait for the natural alignment of the two orbital planes and then perform an in-plane transfer with a small plane change.

The SSO environment introduces a unique challenge for fuel-station deployment. Due to the sun-synchronous condition, the target satellites in an SSO cluster usually exhibit similar RAAN drift rates, since their semi-major axes and inclinations are coordinated to maintain the required solar illumination geometry. Consequently, a fuel station placed directly on the target orbits experiences a very small differential nodal drift, resulting in excessively long natural alignment times. To overcome this limitation, the fuel station orbit can be intentionally offset from the target cluster to generate a favorable J_2-induced drift difference. However, such an orbital offset introduces a trade-off between alignment efficiency and transfer cost, since a larger drift difference may reduce the waiting time but increase the orbital transfer requirements and may violate the inclination compatibility constraints. Therefore, the fuel-station deployment problem requires a coordinated optimization of station orbital parameters and satellite assignments rather than an independent placement or clustering strategy.

1.2 Related Work

On-orbit refueling has been studied from three perspectives. The first perspective concerns mission architectures and enabling techniques. Malyh et al. [7] review representative in-orbit refueling projects and the associated critical techniques.

The second perspective optimizes the service sequence. Chen and Yu [15] study the mission planning of geostationary-orbit refueling under a mixed strategy. Li and Xu [16] address the scheduling of multiple SSO satellites and show that the service sequence depends strongly on the orbital distribution and the mission timing. Zhang et al. [17] study the near-circular LEO multi-spacecraft refueling problem by jointly considering the J_2 perturbation and rendezvous time-window constraints. Zhao et al. [18] further investigate LEO cooperative multi-spacecraft refueling optimization under J_2 perturbation, explicitly accounting for the surplus propellant constraint of each target satellite.

The third perspective optimizes the infrastructure deployment. Zhu et al. [19] formulate the station-arrangement problem for multiple geostationary spacecraft as a facility location-allocation problem. In a subsequent study, they determine the orbit of a fuel station for multiple SSO spacecraft under the J_2 perturbation [20]. Shimane et al. [14] formulate an orbital facility location problem for placing servicing depots for satellite constellations. Han et al. [21] propose a two-stage framework that simultaneously designs the fuel-station orbit and schedules the refueling mission in SSO under the J_2 perturbation, using spectral clustering combined with nonlinear programming for station assignment. Kim et al. [22] further address the co-optimization of depot locations and servicing sequences for satellite constellations with low-thrust transfers, including sensitivity analysis on J_2-induced RAAN drift. For the outer search over mixed continuous-discrete design spaces, particle swarm optimization [23, 24] has been applied to spacecraft refueling scheduling [25] and multi-orbit on-orbit servicing routing [26].

1.3 Contributions

The main contributions of this paper are:

1) A J_2-aware joint optimization framework is proposed for fuel-station orbit design and satellite assignment. Unlike prior two-stage approaches [21] that decouple orbit design from assignment, the proposed approach simultaneously optimizes continuous orbital parameters and discrete target associations within a single PSO search, and explicitly accounts for endpoint-aware return geometry by using the terminal RAAN separation after the service interval.

2) A multi-objective optimization framework is established to balance propellant consumption, cluster-size balance, servicing-spacecraft requirements, and constraint feasibility, which enables trade-offs among these objectives.

2 System Model

2.1 Mission Architecture

The mission contains K fuel stations, a servicing-spacecraft (SSC) resource pool, and N target satellites. A station stores propellant. An SSC loads propellant at a station, transfers to one target, delivers the demanded fuel, and returns to the station. Each SSC executes at most one task at a time and is occupied for a fixed service interval t_{op} per task.

The state of target j is

$$x_j = [a_j, e_j, i_j, \Omega_j, \omega_j, M_j, q_j, R_j], \tag{1}$$

where the first six entries are the classical orbital elements, q_j is the delivered propellant demand, and R_j is the initial residual propellant. The residual propellant of target j is consumed at a constant rate d_j (kg/day), so that it is depleted at R_j/d_j.

The fuel-station orbital parameters are represented as

$$p_k = [a_k^F, i_k^F, \Omega_k^F], \tag{2}$$

where the near-circular assumption removes the eccentricity and the argument of perigee from the parameter vector, and the mean anomaly does not affect the plane geometry.

2.2 J_2 Perturbation and Natural Alignment

The secular variation of the RAAN caused by the J_2 perturbation is approximated as [12]

$$\dot{\Omega} = -9.964 \left(\frac{R_e}{a}\right)^{3.5} \frac{\cos i}{(1-e^2)^2}, \tag{3}$$

where $\dot{\Omega}$ is expressed in deg/day; $R_e = 6378.137$ km is the Earth's equatorial radius; and a, e, and i denote the semi-major axis (km), eccentricity, and inclination, respectively. For near-circular orbits,

$$\dot{\Omega} = -9.964 \left(\frac{R_e}{a}\right)^{3.5} \cos i. \tag{4}$$

For a fuel station k and a target satellite j, the differential nodal drift rate is defined as

$$\Delta\dot{\Omega}_{jk} = \dot{\Omega}_k^F - \dot{\Omega}_j, \tag{5}$$

which determines the evolution of their relative RAAN separation:

$$\Delta\Omega_{jk}(t) = \Omega_k^F(t) - \Omega_j(t). \tag{6}$$

The first natural alignment time is obtained as

$$t_{\text{align}} = \frac{\operatorname{mod}\left(-\operatorname{sgn}(\Delta\dot{\Omega}_{jk})\,\Delta\Omega_{jk}(0),\, 360^\circ\right)}{|\Delta\dot{\Omega}_{jk}|}, \tag{7}$$

where the wrapped RAAN separation is constrained within $[0, 360^\circ)$.

Eq. (7) indicates that the natural alignment capability is primarily governed by the differential RAAN drift rate. Therefore, instead of placing the fuel station directly on the target orbit, an appropriate orbital offset can be introduced to generate a controllable nodal drift difference and reduce the alignment time.

2.3 Transfer and Fuel-Consumption Model

The transfer combines an in-plane Hohmann transfer and an out-of-plane plane change [12]. With μ denoting the gravitational parameter of the Earth, the in-plane increment between a_k^F and a_j is

$$\begin{aligned}\Delta V_T = &\left|\sqrt{\frac{\mu}{a_k^F}}\left(\sqrt{\frac{2a_j}{a_k^F + a_j}} - 1\right)\right| \\ &+ \left|\sqrt{\frac{\mu}{a_j}}\left(1 - \sqrt{\frac{2a_k^F}{a_k^F + a_j}}\right)\right|.\end{aligned} \tag{8}$$

For a plane separation γ, the out-of-plane increment is

$$\Delta V_\perp = 2\sqrt{\frac{\mu}{a_k^F}} \sin\left(\frac{\gamma}{2}\right), \tag{9}$$

$$\gamma = \sqrt{(i_j - i_k^F)^2 + \Delta\Omega^2}, \tag{10}$$

where $\Delta\Omega$ is the RAAN separation at the maneuver epoch. Eq. (10) is a small-angle approximation of the dihedral angle between the two orbital planes and is adequate for the separations considered here. When the station waits for the natural alignment, the departure separation is zero and γ contains only the inclination difference. When the station forces an immediate transfer, γ also contains the current RAAN separation. Each one-way increment is the sum of the in-plane and out-of-plane components, i.e., $\Delta V_{\text{out}} = \Delta V_T + \Delta V_\perp(\gamma_{\text{out}})$ and $\Delta V_{\text{ret}} = \Delta V_T + \Delta V_\perp(\gamma_{\text{ret}})$.

The service interval lasts t_{op} days. During this interval the station and the target keep precessing, so the return maneuver uses the terminal separation instead of the departure separation. We denote the one-way increments by ΔV_{out} and ΔV_{ret}. The propellant cost of one round trip is [20]

$$c_{jk} = m_{\text{dry}} \left[\exp\left(\frac{\Delta V_{\text{out}} + \Delta V_{\text{ret}}}{I_{sp} g_0} \right) - 1 \right] + q_j \left[\exp\left(\frac{\Delta V_{\text{out}}}{I_{sp} g_0} \right) - 1 \right], \tag{11}$$

where m_{dry} is the dry mass of the SSC, I_{sp} is the specific impulse, and g_0 is the standard gravity. The first term accounts for the dry-mass maneuver, and the second term accounts for the transported demand. Eq. (11) follows from applying the rocket equation backward from the return leg: the return consumes $m_{\text{dry}}[\exp(\Delta V_{\text{ret}}/(I_{sp} g_0)) - 1]$, and the outbound leg must carry and accelerate a total mass of $m_{\text{dry}} \exp(\Delta V_{\text{ret}}/(I_{sp} g_0)) + q_j$. All velocity increments are expressed in m/s, consistent with $I_{sp} g_0$.

3 Integrated Optimization Framework

The proposed framework aims to optimize the fuel-station deployment for SSO satellite clusters by jointly considering station orbital parameters and satellite assignments. The optimization process consists of two interacting components: an outer optimization module and an inner mission evaluation module: 1) The outer module searches for the fuel-station orbital configurations and satellite-to-station assignments. 2) For each candidate solution, the inner module evaluates the corresponding refueling performance by determining feasible servicing opportunities, estimating transfer costs, and calculating the multi-objective function. The evaluation process considers the J_2-induced differential nodal drift, natural alignment opportunities, service-duration effects, and operational constraints.

Through this optimization-evaluation interaction, the proposed strategy identifies fuel-station configurations that achieve favorable orbital compatibility with the target satellites while reducing refueling costs and maintaining mission feasibility.

3.1 Problem Statement and Constraints

The design vector contains the station orbits and the assignment,

$$\mathcal{X} = \{p_1, \dots, p_K, y_1, \dots, y_N\}, \quad y_j \in \{1, \dots, K\}, \tag{12}$$

where p_k denotes the orbital parameters of fuel station k, and y_j represents the station assigned to target satellite j. The optimization minimizes the multi-objective J in Eq. (28), subject to six constraints:

1) Each target belongs to exactly one station.

2) The station inclination stays close to every assigned target,

$$y_j = k \Rightarrow |i_j - i_k^F| \le \Delta i_{\max}. \tag{13}$$

3) A task starts before the residual fuel runs out

$$t_{\text{dep}} < \frac{R_j}{d_j} \tag{14}$$

4) Each task finishes within the horizon,

$$t_{\text{dep}} + t_{\text{op}} \le T_{\text{mission}} \tag{15}$$

5) Each SSC serves at most one target at a time, which the scheduler enforces through a sequential free-time variable t_{free}.

6) The terminal RAAN separation after the service interval remains within the allowable limit,

$$|\Delta\Omega_{jk}(t_{\text{dep}} + t_{\text{op}})| \le \Delta\Omega_{\max}. \tag{16}$$

Constraints (1) and (2) characterize the deployment, while (3)–(6) couple the deployment with the schedule. Constraints (2) and (3) interact through the inclination offset. A small offset produces a small differential drift rate and a long alignment time, so the fuel deadline imposes a lower bound on the offset. A large offset improves the alignment but violates the compatibility of the far targets in the cluster. Because the station has a single inclination shared by all targets, the assignment determines how well one offset serves the whole cluster. This coupling is the reason a decoupled procedure is restrictive, and it motivates the integrated treatment below.

3.2 Deterministic Service Evaluation Strategy

For a given fuel-station deployment and satellite assignment, the evaluation procedure determines the feasible service sequence and computes the associated fuel consumption and SSC requirement. For each station and its assigned cluster, the targets are processed according to their natural alignment times obtained from Eq. (7). Each nonempty station is initially equipped with one primary SSC with availability time $t_{\text{free}} = 0$.

With the relative RAAN separation $\Delta\Omega_{jk}(t)$ defined in Eq. (6), natural alignment is achieved when

$$\Delta\Omega_{jk}(t) \equiv 0 \pmod{360^\circ}. \tag{17}$$

For a nonzero differential nodal drift rate, the alignment period is

$$P = \frac{360^\circ}{|\Delta\dot{\Omega}_{jk}|}. \tag{18}$$

The next available alignment epoch after t_{free} is

$$t_{\text{align}}^{\text{next}}(j) = t_{\text{align}}(j) + n_j P, \tag{19}$$

where

$$n_j = \left\lceil \frac{\max(0, t_{\text{free}} - t_{\text{align}}(j))}{P} \right\rceil. \tag{20}$$

The primary SSC departure time is therefore

$$t_{\text{dep}} = \max\left(t_{\text{free}}, t_{\text{align}}^{\text{next}}(j)\right). \tag{21}$$

A task is feasible if the departure time satisfies the fuel deadline and mission horizon constraints, and the terminal RAAN separation after the service interval remains within the allowable limit:

$$\begin{aligned} t_{\text{dep}} &< R_j/d_j, \\ t_{\text{dep}} + t_{\text{op}} &\le T_{\text{mission}}, \\ |\Delta\Omega_{jk}(t_{\text{dep}} + t_{\text{op}})| &\le \Delta\Omega_{\max}. \end{aligned} \tag{22}$$

The outbound transfer uses the aligned departure geometry,

$$\gamma_{\text{out}} = |i_j - i_k^F|, \tag{23}$$

while the return transfer accounts for the terminal RAAN drift,

$$\gamma_{\text{ret}} = \sqrt{(i_j - i_k^F)^2 + \Delta\Omega_{jk}^2(t_{\text{dep}} + t_{\text{op}})}. \tag{24}$$

The task fuel consumption c_{jk} is calculated from Eq. (11). If the primary SSC cannot satisfy the above constraints, an additional SSC is introduced at the same station and assigned to the first feasible alignment opportunity. Such an SSC increases the station-level SSC requirement but does not modify the availability of the primary SSC. Tasks that cannot be completed contribute to the aggregate violation V.

The SSC requirement of station k is calculated as

$$N_{\text{SSC},k} = 1 + n_{\text{add},k}, \tag{25}$$

and the resulting N_{SSC} and V are included in the objective function in Eq. (28).

3.3 Multi-Objective Optimization Formulation

For each candidate deployment solution, the mission evaluation procedure calculates the propellant consumption associated with all refueling tasks. The total fuel consumption is defined as

$$C_{\text{fuel}} = \sum_k \sum_{j \in \mathcal{C}_k} c_{jk}, \tag{26}$$

where $\mathcal{C}_k$ denotes the set of target satellites assigned to fuel station k, and c_{jk} represents the fuel required for servicing target j.

In addition to fuel consumption, the deployment strategy should maintain a balanced distribution of targets among fuel stations. Therefore, the cluster-size dispersion is introduced as

$$\Phi_{\text{size}} = \frac{\text{std}(n_1, \ldots, n_K)}{\text{mean}(n_1, \ldots, n_K)}, \tag{27}$$

where $n_k = |\mathcal{C}_k|$ denotes the number of targets assigned to station k. A smaller value of Φ_{size} indicates a more balanced workload distribution among fuel stations.

The number of required servicing spacecraft is represented by N_{SSC}. In the current formulation, each nonempty fuel station requires one servicing spacecraft, and an additional spacecraft is introduced when consecutive transfers cannot be performed by the same vehicle due to operational constraints.

Considering the above factors, a multi-objective cost function is formulated as

$$\begin{aligned} J = w_f \frac{C_{\text{fuel}}}{C_{\text{ref}}} + w_s \frac{\Phi_{\text{size}}}{S_{\text{ref}}} + w_{\text{ssc}} \frac{N_{\text{SSC}}}{N_{\text{SSC,ref}}} \\ + w_v \frac{V}{V_{\text{ref}}}, \end{aligned} \tag{28}$$

where V represents the aggregated constraint violation. The reference values C_{ref}, S_{ref}, $N_{\text{SSC,ref}}$, and V_{ref} are introduced to normalize different objectives with distinct physical units, allowing the weighting coefficients to remain dimensionless and comparable. Eq. (28) is a weighted-sum scalarization of the multiple objectives; therefore, each weight setting yields one compromise solution rather than the full Pareto front.

The optimization therefore seeks a fuel-station deployment and satellite assignment strategy that minimizes propellant consumption while maintaining balanced station utilization, reasonable servicing spacecraft requirements, and operational feasibility.

3.4 Particle Swarm Optimization for Joint Placement and Assignment

The proposed optimization problem involves both continuous orbital variables and discrete assignment variables. To address this problem, a particle swarm optimizer (PSO) [23, 24] is adopted as the outer search algorithm, which has demonstrated effectiveness in spacecraft refueling scheduling problems [25]. The scheduling subproblem addressed here is also related to multi-orbit on-orbit servicing routing and scheduling [26].

The station orbital parameters are directly encoded as continuous variables, while the discrete assignment variables are represented using a continuous encoding scheme to enable PSO optimization. Specifically, each assignment variable is mapped from $\tilde{y}_j \in [0, 1)$ to an integer station index according to

$$y_j = 1 + \lfloor \tilde{y}_j K \rfloor. \tag{29}$$

After decoding, a repair procedure is applied to restore feasibility when the inclination compatibility constraint is violated. In this process, the affected satellite is reassigned to the nearest feasible fuel station. Solutions with unused fuel stations are discarded because each optimized station is assumed to participate in the servicing mission.

To improve convergence efficiency, an informed initial particle is generated before the PSO search. The initial solution first groups target satellites according to their inclination and RAAN distributions, and then determines preliminary station orbits that provide suitable differential nodal drift rates based on the natural alignment relationship in Eq. (7). The remaining particles are initialized using random samples and small perturbations around the initial solution to maintain a balance between global exploration and local refinement. For infeasible solutions, a finite penalty value is added to the objective function rather than assigning an infinite cost. This penalty strategy provides a gradual preference toward feasible regions and avoids eliminating potentially promising solutions during the early search stage.

4 Simulation and Results

4.1 Simulation Setup

The numerical study uses a 20-target SSO cluster. Table 1 lists the orbital elements, the demand q_j, and the residual fuel R_j. The mission horizon is $T_{\text{mission}} = 1095$ days, each task lasts $t_{\text{op}} = 30$ days, and the number of stations is $K = 3$. The inclination-compatibility limit is $\Delta i_{\max} = 4°$. The propulsion parameters are $m_{\text{dry}} = 150$ kg and $I_{sp}g_0 = 3200$ m/s. The residual-propellant consumption rate is $d_j = 0.03$ kg/day for all targets. With this rate, the smallest fuel deadline in Table 1 is $R_5/d_5 = 1700$ days, which exceeds T_{mission}; hence, in this case study the mission horizon, rather than the fuel deadline, is the binding timing constraint. The maximum allowable terminal RAAN separation is set to $\Delta\Omega_{\max} = 5°$, which bounds the return-leg plane-change cost to a level consistent with the propulsion budget.

Table 1. Initial orbital parameters and fuel status of the 20 target satellites.

ID	a (km)	i (°)	Ω (°)	q (kg)	R (kg)
1	6628.0	96.5	221.1	190	87
2	6769.1	97.0	188.3	220	84
3	6825.3	97.2	12.4	230	119
4	6876.9	97.4	235.0	170	226
5	6980.5	97.8	74.7	250	51
6	7055.6	98.1	194.1	140	162
7	7104.6	98.3	149.0	200	194
8	7200.1	98.7	180.3	160	105
9	7447.0	99.8	200.6	240	78
10	7489.7	100.0	191.0	210	147
11	7614.1	100.6	160.2	150	123
12	7713.8	101.1	279.1	250	215
13	7903.6	102.1	3.0	190	62
14	8150.5	103.5	120.3	220	203
15	8283.0	104.3	15.6	230	106
16	8425.4	105.2	330.9	200	129
17	8677.7	106.9	30.0	200	88
18	8706.0	107.1	55.0	220	156
19	8870.9	108.3	35.5	180	64
20	9077.8	109.9	215.1	200	198

4.2 Optimized Deployment

The optimized deployment is summarized in Table 2. The three stations serve 20 targets with cluster sizes of 5, 7, and 8, respectively. The corresponding cluster fuel consumptions are 1467.0 kg, 1128.9 kg, and 809.9 kg, resulting in a total refueling-related fuel consumption of 3405.8 kg.

Table 2. Optimized fuel-station deployment and cluster-level results.

Station	a^F (km)	i^F (°)	Ω^F (°)	n_k	$C_{\text{fuel,k}}$ (kg)	$N_{\text{SSC},k}$
FS1	7736.9	107.86	185.49	5	1467.0	1
FS2	8683.6	102.72	16.34	7	1128.9	1
FS3	7366.3	97.31	240.69	8	809.9	2
Total	–	–	–	20	3405.8	4

The optimized station states exhibit the orbital-offset structure required by the J_2-aware deployment strategy. Each station satisfies the inclination compatibility constraint with its assigned targets while maintaining a nonzero differential nodal drift, which provides natural RAAN alignment opportunities for subsequent servicing tasks.

FS1 and FS2 complete all assigned tasks using one primary SSC, whereas FS3 requires one additional SSC to perform a parallel service operation within the mission horizon. Therefore, the total SSC requirement is four, including one primary SSC for each active station and one additional SSC introduced by the service evaluation procedure.

Figure 1 shows the convergence history of the normalized objective, and Figure 2 presents the final target assignment and fuel-station placement in the inclination–RAAN plane.

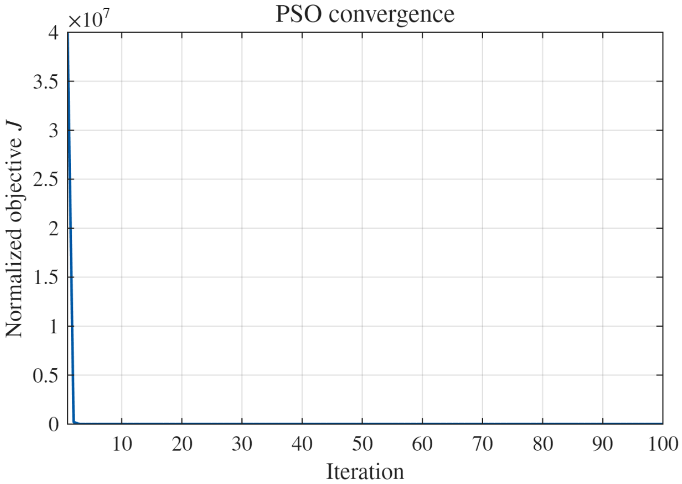

Figure 1. Convergence history of the normalized objective.

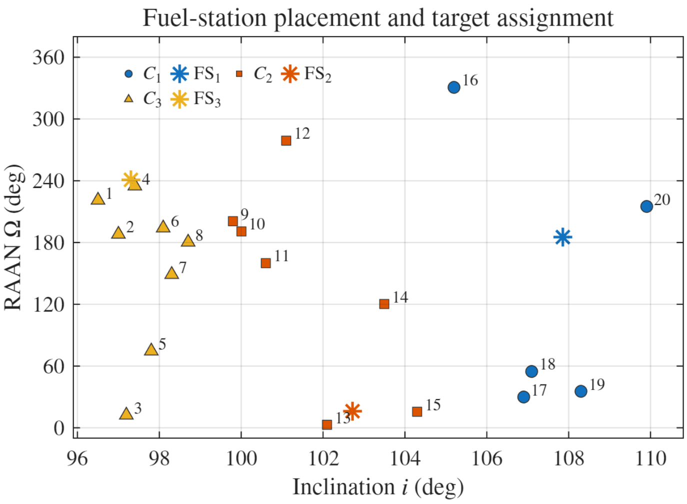

Figure 2. Optimized target assignment and fuel-station placement in the inclination–RAAN plane. The stars indicate the optimized station states.

4.3 Service Schedule and SSC Decisions

The deterministic evaluation procedure generates the service sequence for each optimized fuel station according to the natural alignment opportunities and SSC availability. The resulting departure times, task ordering, and SSC decisions are summarized below.

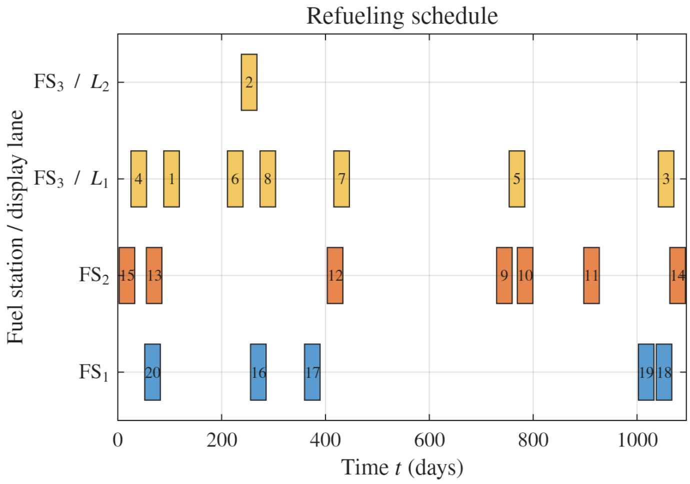

Figure 3. Service schedule of the optimized deployment. Each bar represents one 30-day refueling task, and each row corresponds to one fuel station.

Figure 3 illustrates the obtained service schedule. Each bar represents one refueling task with a fixed duration of $t_{\mathrm{op}} = 30$ days. The three fuel stations complete 20 service tasks over the mission horizon, with departure epochs determined by the J_2-induced natural alignment condition.

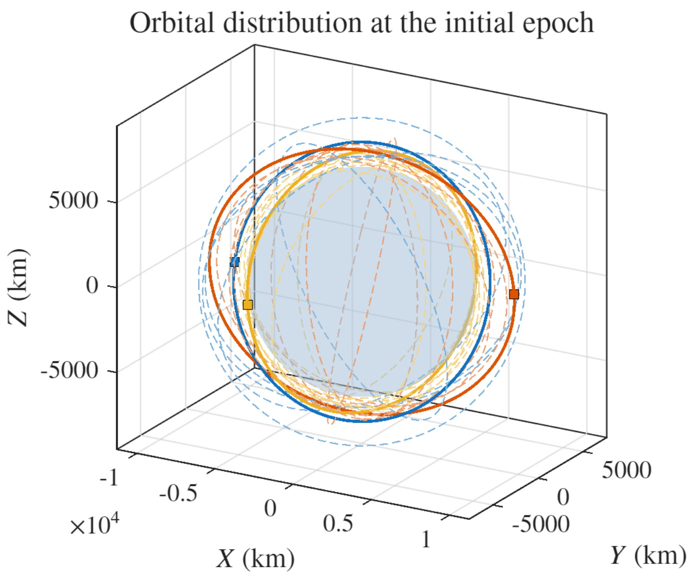

Figure 4. Initial three-dimensional orbital configuration of the SSO cluster and optimized fuel-station orbits.

Most tasks are executed by the primary SSC through naturally aligned departures. As shown in Figure 3, FS1 and FS2 require no additional servicing spacecraft, while FS3 introduces one additional SSC for the fifth task in its assigned sequence. This additional SSC does not change the primary SSC availability but enables the parallel execution required to satisfy the mission constraints. Figure 4 shows the initial 3D orbital configuration of the SSO satellite cluster and the optimized orbits of the refueling stations.

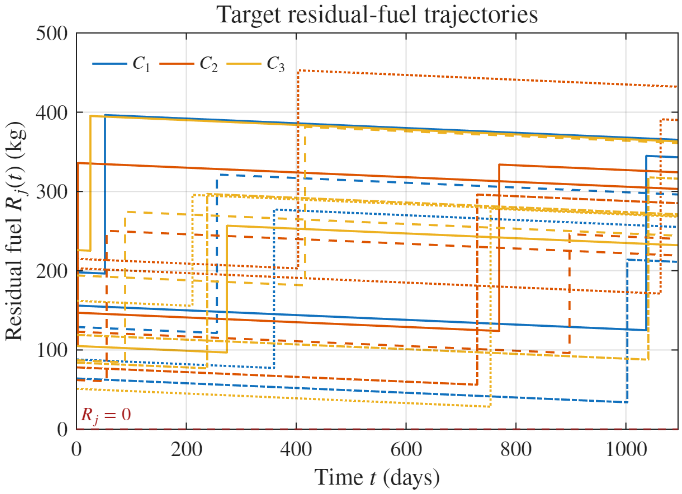

Figure 5. Residual-fuel trajectories of the target satellites. Each jump represents one refueling event.

The residual-fuel evolution of the target satellites is presented in Figure 5. The fuel trajectories show that every target is refueled before its residual propellant is depleted, while accounting for the waiting time introduced by natural alignment.

5 Conclusion

This paper presented a J_2-aware joint optimization framework for fuel station placement and satellite assignment in SSO satellite clusters. The proposed framework integrates PSO-based deployment optimization with a deterministic service evaluation strategy that considers natural RAAN alignment, endpoint-aware transfer geometry, fuel consumption, and SSC requirements. The numerical results demonstrate that the optimized fuel stations maintain appropriate orbital offsets to generate differential RAAN drift while satisfying the inclination compatibility constraint. For the considered 20-target SSO cluster, the obtained three-station deployment provides a feasible servicing solution with four SSCs, including one additional SSC for parallel task execution. The proposed framework provides a systematic approach for analyzing the coupling between orbital configuration, servicing resources, and mission-level objectives. Future research will focus on improving the fidelity, robustness, and scalability of the proposed framework.

Data Availability Statement

Data will be made available on request.

Funding

This work was supported without any funding.

Conflicts of Interest

The authors declare no conflicts of interest.

AI Use Statement

The authors declare that no generative AI was used in the preparation of this manuscript.

Ethical Approval and Consent to Participate

Not applicable.

References

[1] Luu, M. A., & Hastings, D. E. (2022). On-orbit servicing system architectures for proliferated low-Earth-orbit constellations. *Journal of Spacecraft and Rockets, 59*(6), 1946-1965. [CrossRef]

[2] Selva, D., Golkar, A., Korobova, O., Lluch i Cruz, I., Collopy, P., & de Weck, O. L. (2017). Distributed Earth satellite systems: What is needed to move forward? *Journal of Aerospace Information Systems, 14*(8), 412-438. [CrossRef]

[3] Xu, C., Wang, J., & Zhang, C. (2026). Boundary-constrained spacecraft swarm maintenance via periodic reconfiguration in J_2-perturbed near-circular orbits. *Aerospace Science and Technology, 178*, 113046. [CrossRef]

[4] Macdonald, M., McKay, R., Vasile, M., & Frescheville, F. B. D. (2010). Extension of the sun-synchronous orbit. *Journal of Guidance, Control, and Dynamics, 33*(6), 1935-1940. [CrossRef]

[5] Aorpimai, M., & Palmer, P. L. (2007). Repeat-groundtrack orbit acquisition and maintenance for Earth-observation satellites. *Journal of guidance, control, and dynamics, 30*(3), 654-659. [CrossRef]

[6] Zhao, S., Zhang, J., Xiang, K., & Qi, R. (2017). Target sequence optimization for multiple debris rendezvous using low thrust based on characteristics of SSO. *Astrodynamics, 1*(1), 85-99. [CrossRef]

[7] Malyh, D., Vaulin, S., Fedorov, V., Peshkov, R., & Shalashov, M. (2022). A brief review on in-orbit refueling projects and critical techniques. *Aerospace Systems, 5*(2), 185-196. [CrossRef]

[8] Kim, J., Sung, T., Hwang, W., & Ahn, J. (2026). On-Orbit Servicing-Integrated Maintenance Strategy for a Satellite Constellation. *Journal of Spacecraft and Rockets*, 1-18. [CrossRef]

[9] Du Jonchay, T. S., & Ho, K. (2017). Quantification of the responsiveness of on-orbit servicing infrastructure for modularized earth-orbiting platforms. *Acta Astronautica, 132*, 192-203. [CrossRef]

[10] Dutta, A., & Tsiotras, P. (2010). Network flow formulation for cooperative peer-to-peer refueling strategies. *Journal of Guidance, Control, and Dynamics, 33*(5), 1539-1549. [CrossRef]

[11] Meng, B., Huang, J., Li, Z., Huang, L., Pang, Y., Han, X., & Zhang, Z. (2019). The orbit deployment strategy of OOS system for refueling near-earth orbit satellites. *Acta Astronautica, 159*, 486-498. [CrossRef]

[12] Vallado, D. A. (2013). *Fundamentals of Astrodynamics and Applications* (4th ed.). Hawthorne, CA: Microcosm Press. ISBN 978-1-881883-18-0. https://books.google.co.in/books?id=PJLlWzMBKjkC

[13] Zuo, X., Li, K., Chen, L., He, X., & Xu, M. (2025). Fixed-period strategy for maintaining the absolute configuration of large-scale LEO constellations. *Advances in Space Research, 76*(8), 4663-4678. [CrossRef]

[14] Shimane, Y., Gollins, N., & Ho, K. (2024). Orbital facility location problem for satellite constellation servicing depots. *Journal of Spacecraft and Rockets, 61*(3), 808-825. [CrossRef]

[15] Chen, X., & Yu, J. (2017). Optimal mission planning of GEO on-orbit refueling in mixed strategy. *Acta Astronautica, 133*, 63-72. [CrossRef]

[16] Li, C., & Xu, B. (2020). Optimal scheduling of multiple Sun-synchronous orbit satellites refueling. *Advances in Space Research, 66*(2), 345-358. [CrossRef]

[17] Zhang, J., Parks, G. T., Luo, Y., & Tang, G. (2014). Multispacecraft refueling optimization considering the J_2 perturbation and window constraints. *Journal of Guidance, Control, and Dynamics, 37*(1), 111-122. [CrossRef]

[18] Zhao, Z., Zhang, J., Li, H., & Zhou, J. (2017). LEO cooperative multi-spacecraft refueling mission optimization considering J_2 perturbation and target's surplus propellant constraint. *Advances in Space Research, 59*(1), 252-262. [CrossRef]

[19] Zhu, X., Chen, J., Zhang, C., & Qiao, B. (2020). Optimal fuel station arrangement for multiple GEO spacecraft refueling mission. *Advances in Space Research, 66*(8), 1924-1936. [CrossRef]

[20] Zhu, X., Zhang, C., Sun, R., Chen, J., & Wan, X. (2020). Orbit determination for fuel station in multiple SSO spacecraft refueling considering the J_2 perturbation. *Aerospace Science and Technology, 105*, 105994. [CrossRef]

[21] Han, P., Guo, Y., Wang, P., Li, C., & Pedrycz, W. (2023). Optimal orbit design and mission scheduling for Sun-synchronous orbit on-orbit refueling system. *IEEE Transactions on Aerospace and Electronic Systems, 59*(5), 4968-4983. [CrossRef]

[22] Kim, J., Shimane, Y., & Ho, K. (2025). Orbital depot location optimization for satellite constellation servicing with low-thrust transfers. *Journal of Spacecraft and Rockets*. [CrossRef]

[23] Kennedy, J., & Eberhart, R. (1995). Particle swarm optimization. In *Proceedings of ICNN'95 - International Conference on Neural Networks* (Vol. 4, pp. 1942-1948). [CrossRef]

[24] Shi, Y., & Eberhart, R. (1998, May). A modified particle swarm optimizer. In *Evolutionary computation proceedings* (Vol. 890, pp. 69-73). [CrossRef]

[25] Zhou, Y., Yan, Y., Huang, X., & Kong, L. (2015). Optimal scheduling of multiple geosynchronous satellites refueling based on a hybrid particle swarm optimizer. *Aerospace Science and Technology, 47*, 125-134. [CrossRef]

[26] Sorenson, S. E., & Pinkley, S. G. N. (2023). Multi-orbit routing and scheduling of refuellable on-orbit servicing space robots. *Computers & Industrial Engineering, 176*, 108852. [CrossRef]